PCCP

PAPER

View Article Online
View Journal | View Issue

Cite this: *Phys. Chem. Chem. Phys.*, 2020, **22**, 1715

Optimizing photon upconversion by decoupling excimer formation and triplet triplet annihilation†

Chen Ye,[a] Victor Gray,[bc] Khushbu Kushwaha,[a] Sandeep Kumar Singh,[d] Paul Erhart[d] and Karl Börjesson *[a]

Received 4th December 2019,
Accepted 18th December 2019

DOI: 10.1039/c9cp06561j

rsc.li/pccp

Perylene is a promising annihilator candidate for triplet–triplet annihilation photon upconversion, which has been successfully used in solar cells and in photocatalysis. Perylene can, however, form excimers, reducing the energy conversion efficiency and hindering further development of TTA-UC systems. Alkyl substitution of perylene can suppress excimer formation, but decelerate triplet energy transfer and triplet–triplet annihilation at the same time. Our results show that mono-substitution with small alkyl groups selectively blocks excimer formation without severly compromising the TTA-UC efficiency. The experimental results are complemented by DFT calculations, which demonstrate that excimer formation is suppressed by steric repulsion. The results demonstrate how the chemical structure can be modified to block unwanted intermolecular excited state relaxation pathways with minimal effect on the preferred ones.

Introduction

Triplet–triplet annihilation photon upconversion (TTA-UC) can help light harvesting materials to overcome their bandgap limitation and thus achieve higher solar energy conversion efficiencies beyond the Shockley–Queisser limit.[1–7] The mechanism has recently been successfully incorporated in solar cells,[8–14] photocatalysts,[15–18] optical devices,[19–24] and light imaging.[25–31] It requires two functional species, a sensitizer and an annihilator. The sensitizer absorbs a photon and transfers the energy to an annihilator through triplet energy transfer.[32] Two annihilator molecules in their triplet excited states undergo triplet–triplet annihilation[29] upon close contact, promoting one molecule to its excited singlet state from where emission of a high energy photon occurs. Perylene is among the most promising annihilator candidates due to its high stability, commercial availability, and excellent photo-physical properties.[34] TTA-UC systems based on perylene as the annihilator hold the photon upconversion quantum yield record and have now been used in solar cells, photo-redox catalysis and bio-imaging.[18,35–37]

The drawback of perylene is its tendency to form excited dimers (excimers). Excimer formation in TTA-UC reduces the overall energy conversion efficiency, both due to the lower energy of the emitted photons and due to the significant rate constant of non-radiative decay from excimers.[38] Dover *et al.* have shown the conversion between monomers and excimers through triplet pair and free diffusion during both singlet fission and TTA-UC.[39] We have further suggested that another main reason for the surprisingly large amount of excimer emission in perylene based photon upconversion is due to a preassembly step on the triplet energy surface, already before the upconversion event.[40] Alkyl substitution offers the opportunity to manipulate the stacking interactions of perylene with minimal impact on the excited levels of the individual molecules. Indeed, perylene derivatives like tetra-*tert*-butyl-perylene show low excimer formation in TTA-UC, since the molecular aggregation is sterically hindered.[41,42] However, the steric bulk also reduces mobility and molecular contact, and thus can inhibit triplet energy transfer[32,43] and TTA. It is therefore of great importance to control the pi–pi interactions in perylene in order to limit excimer formation without compromising photon upconversion performance.

Here, a series of alkyl substituted perylene derivatives are used to investigate the interplay between upconversion performance and excimer formation blockade. Static and dynamic upconversion experiments show that an ethyl group is sufficient to block excimer formation. This result is corroborated by calculations, which show that steric hindrance prevents coupling on the excimer landscape. The results presented here shed light on molecular design of TTA-UC annihilators and help to optimize annihilator molecules for TTA-UC.

[a] *Department of Chemistry and Molecular Biology, University of Gothenburg, 41296 Gothenburg, Sweden. E-mail: karl.borjesson@gu.se*
[b] *Department of Chemistry–Ångström Laboratory, Uppsala University, 75120, Uppsala, Sweden*
[c] *Department of Physics, Cavendish Laboratory, University of Cambridge, 19 JJ Thompson Avenue, Cambridge, CB3 0HE, UK*
[d] *Department of Physics, Chalmers University of Technology, 41296 Gothenburg, Sweden*

† Electronic supplementary information (ESI) available. See DOI: 10.1039/c9cp06561j

Results

Spectroscopic characterization of annihilators

To assess the effect of increasing steric hindrance on excimer formation and upconversion efficiency, four perylene derivatives were used: perylene (**pery**), 1-ethyl-perylene (**et-pery**), 3-*tert*-butyl-perylene (***t*-bu-pery**) and 2,5,8,11-tetra-*tert*-butylperylene (**t-*t*-bu-pery**), which are available from our previous work (Fig. 1a).[44] The absorption and emission spectra of these molecules in tetrahydrofuran (THF) are shown in Fig. 1b revealing only minor changes to the energy of the singlet excited state. The Stokes shifts of **pery**, **et-pery**, ***t*-bu-pery** and **t-*t*-bu-pery** are 103 cm^{-1}, 736 cm^{-1}, 938 cm^{-1} and 849 cm^{-1}, respectively. The increased Stokes shift after alkyl substitution indicates that the difference in polarizability between the ground and excited states increases when alkylated.[45] All four annihilators demonstrate fluorescence quantum yields near unity, and a fluorescence lifetime of 3.8 ns, indicating that the excited states configuration is not affected much by the substitution (Fig. S1, ESI†).

Photon upconversion with different annihilators

In order to construct TTA-UC systems with these perylene derivatives, we used Platinum tetra-benzo-tetra-phenyl-porphyrin (PtTBTP) as a triplet sensitizer. PtTBTP has a high phosphorescence quantum yield, long triplet lifetime, and a triplet energy that matches the one of perylene.[46] The potential photon energy increase of the PtTBTP/perylene couple is 0.75 to 0.83 eV, as determined by the difference of the E_{00} energies (Fig. S2, ESI†).[47] Photon upconversion using PtTBTP in combination with the presented perylene derivatives was performed using a light-emitting diode (LED) as excitation source (617 nm; Fig. 1c). For all perylene derivatives, strong emission can be observed in the range 450 nm to 540 nm, which is assigned to perylene fluorescence due to TTA-UC. Excimer emission at 565 nm from perylene is also present.[48] The quantum yield of excimer emission increases with perylene concentration, indicating a process for perylene excimer formation that involves diffusion. No excimer emission was, however, observed for the three perylene derivatives with steric side groups over a wide range of annihilator concentrations (Fig. 1d). We can thus conclude that even such small substituents as an ethyl group are enough to block excimer formation in perylene derivatives. Photon-upconversion emission of the four annihilators show linear and quadratic dependence on the excitation intensity (Fig. S3, ESI†), as a typical feature of TTA-UC. The light intensity threshold of quadratic to linear dependence increases after alkyl substitution, reducing the TTA-UC efficiency at low excitation intensity.

Energetics of annihilator dimers

It has recently been suggested that a reason for strong excimer emission in perylene based TTA-UC is the formation of excimers on the triplet surfaces before the annihilation event.[40] The relationship between excimer formation and molecular structure can be explored from an energetic point of view (Note S1.6, ESI†). To this end, we analysed the potential energy surface for the interaction between a pair of perylene molecules within the framework of time-dependent density functional theory (TD-DFT).[49–52] We relaxed the structure of the molecular dimers on the ground state (S_0) potential energy surface (PES). Subsequently, we mapped out the PES as a function of the lateral displacement of the two monomers (Fig. 2a and b). The z offset distances for **pery** and **et-pery** are about 3.32 and 3.48 Å, respectively. The first excited singlet (S_1) and triplet (T_1) energy surfaces of the dimer were then created by adding the respective excitation energies to the ground state energy.

In the ground state of the **pery** dimer, the two monomers are shifted relative to each other, similar to the situation in a graphene bilayer.[53] The singlet and triplet excimers on the other hand, are characterized by perfect lateral alignment of the two monomers. The energies of the two configurations

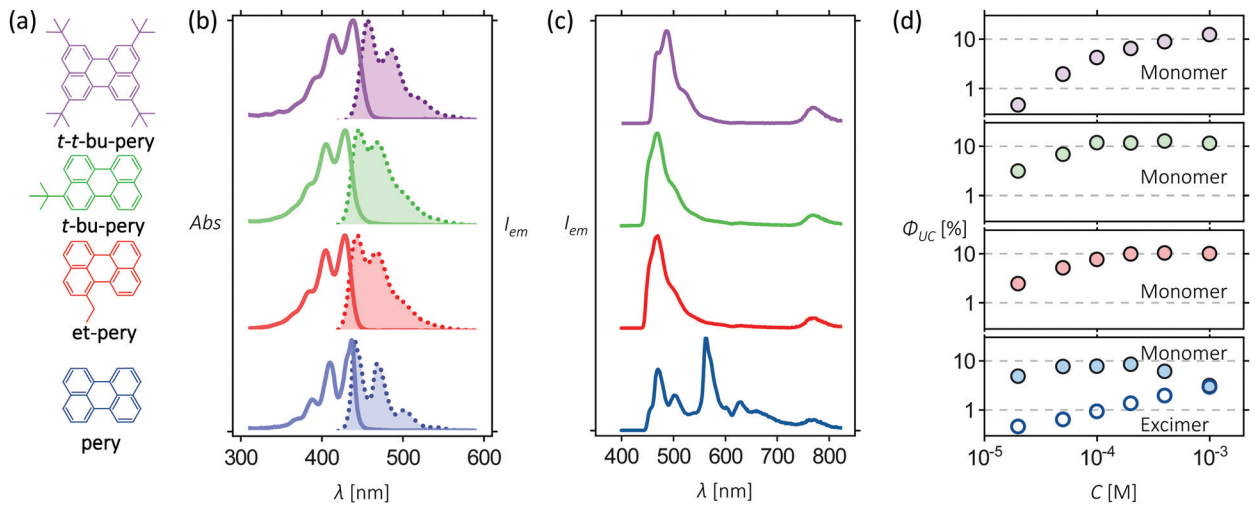

Fig. 1 (a) Molecular structure of **pery**, **et-pery**, ***t*-bu-pery**, and **t-*t*-bu-pery**; (b) absorption/emission spectra of 10 μM **pery**, **et-pery**, ***t*-bu-pery**, and **t-*t*-bu-pery** in THF when excited at 400 nm; (c) upconverted emission spectra from solutions of 10 μM PtTBTP and 1 mM perylene derivatives upon excitation at 617 nm in THF.[33] The absolute photon upconversion quantum yields at different concentrations of annihilators.

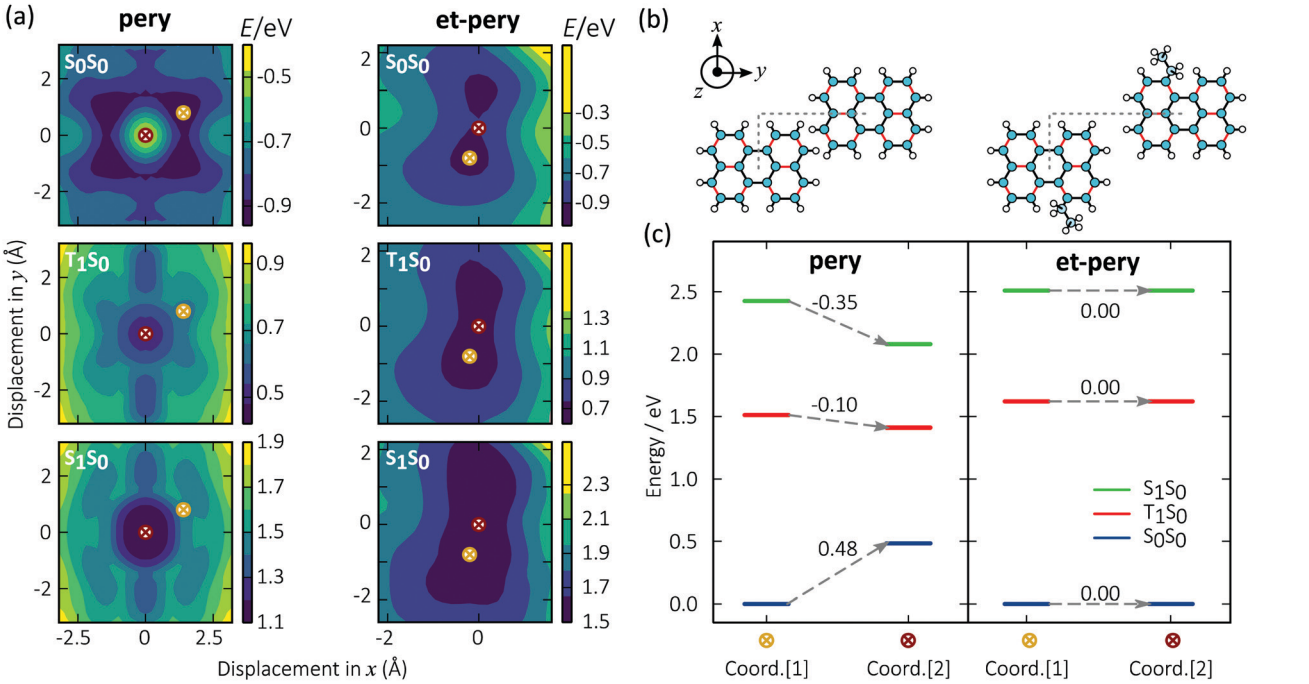

Fig. 2 (a) Calculated energy surfaces of the confined systems of **pery** and **et-pery** dimers. The energy minimum geometry on the S_0S_0 energy surface is labelled with a yellow cross, and the energy minimum geometry on the T_1S_0 and S_1S_0 energy surfaces is labelled with a red cross; (b) bi-molecular coordination of **pery** and **et-pery** dimer on *xy* plane; (c) energy diagram of **pery** and **et-pery** dimer at relaxation.

differ by 0.48 eV, −0.10 eV, and −0.35 eV on the S_0, T_1, and S_1 surfaces, respectively. These energy differences correlates with low energy excimer emission (Fig. 2c).

The PES of **et-pery** is less symmetric than in the case of **pery** and the lowest energy configurations on the S_0, T_1, and S_1 landscape are almost identical to each other. The distortion of the molecular geometry caused by the et groups impacts the ability of the two monomers to move relative to each other (note that the core of **et-pery** is slightly twisted). This prevents them from achieving an alignment that, as in the case of **pery**, enables efficient coupling on the excited landscape, and thus excimer formation. We can conclude that alkyl substitution is an effective means to disrupt the favourable excimer geometry of perylene on both singlet and triplet energy surfaces.

Kinetics of photon upconversion

While alkyl substitution prevents excimer formation, it also has drawbacks. Increasing the molecular size by alkylation reduces the molecular mobility and thus the bimolecular reaction rates of triplet energy transfer[32] and TTA. The TET rate constant can be determined by examining the quenching efficiency of the sensitizer phosphorescence by the annihilator. The relationship between the quenching effect and quencher concentration follows the Stern–Volmer equation (eqn (1) and (2)).[54]

$$\frac{\tau_0}{\tau} = 1 + K_{SV}[A] = 1 + k_{TET}\tau_0[A] \quad (1)$$

$$\Phi_{TET} = \frac{k_{TET}\tau_0[A]}{1 + k_{TET}\tau_0[A]} \quad (2)$$

In eqn (1) and (2), τ_0 is the phosphorescence lifetime of the sensitizer in absence of an annihilator, τ is the lifetime of the sensitizer in presence of an annihilator, K_{SV} is the Stern–Volmer constant, k_{TET} is the TET rate constant, and [A] is the concentration of the annihilator. Fig. 3a displays the sensitizer quenching as the concentration of annihilator is increased. With increasing alkyl substitution, the rate of TET is decreasing. It is instructive to compare the TET quantum yield (Φ_{TET}) as a function of annihilator concentration calculated by eqn (2) (Fig. 3b). To reach a TET quantum efficiency of 0.99, the concentration of **pery**, **et-pery**, ***t*-bu-pery**, and **t-*t*-bu-pery** should be 1.0, 2.2, 2.6 and 11.5 mM, respectively. The relatively low TET efficiency of **t-*t*-bu-pery** thus requires highly concentrated conditions to quench the triplet sensitizer effectively. This effect is directly related to the bigger molecular size and the steric hindrance caused by the substitution. Therefore, as small substitution as possible is preferable in order to maintain a high TET efficiency.

Alkyl substitution will not only affect the rate of TET, also the rate of TTA will be affected. The generation of annihilators in the excited triplet state is on the timescale of a few hundereds of nanoseconds to a few microseconds, whereas consumption is on the microsecond timescale. We can then describe the kinetics of TTA-UC by the following equations (eqn (3) and (4)), which assume that the annihilators are in the triplet excited state to start with:

$$\frac{\partial[^3A^*]}{\partial t} = -2k_{TTA}[^3A^*]^2 - k_T[^3A^*] \quad (3)$$

$$\frac{\partial[^1A^*]}{\partial t} = k_{TTA}[^3A^*]^2 - k_F[^1A^*] \quad (4)$$

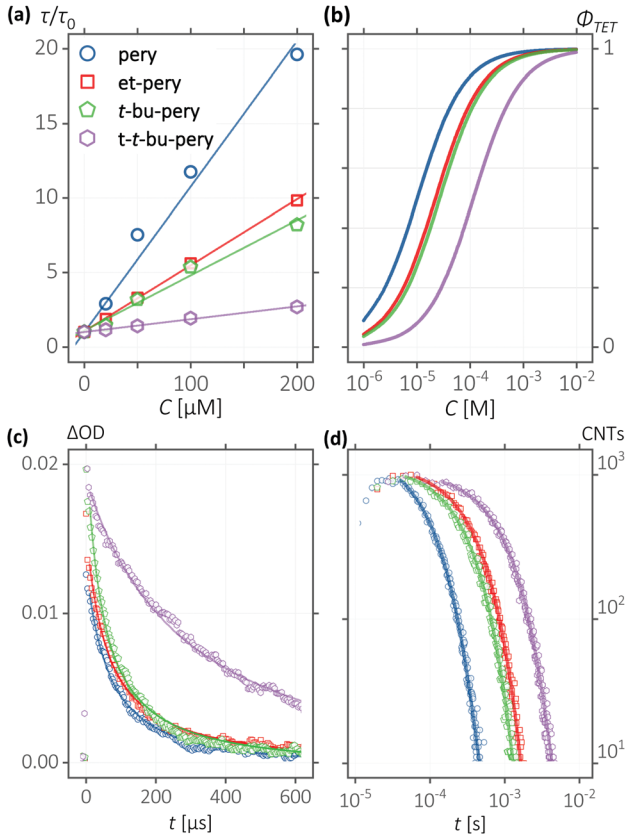

Fig. 3 (a) Stern–Volmer quenching relationship of PtTBTP sensitizer and perylene derivatives; (b) simulated triplet energy transfer efficiencies; (c) time resolved transient absorption decay at the of annihilator $T_1 \rightarrow T_n$ transition peaks of 10 μM PtTBTP and 1 mM perylene/perylene derivatives in THF when excited at 617 nm with pulse energies between 0.30 and 0.37 mJ; (d) time-resolved delayed fluorescence decay at 470 nm of 10 μM PtTBTP and 1 mM perylene/perylene derivatives in THF when excited at 617 nm with pulse energies of 4 μJ.

where $[^3A^*]$ and $[^1A^*]$ are the concentrations of annihilator in the excited triplet and singlet states, respectively, t is the time after excitation, k_{TTA} is the TTA rate constant, k_T is the intrinsic decay rate constant of the excited triplet annihilator, and k_F is the fluorescence decay rate constant of the excited singlet annihilator.[55,56]

The kinetics of the triplet excited annihilator was measured by transient absorption. The triplet states were monitored by their T_1 to T_n transitions (Fig. S4, ESI†). Fig. 3c displays the time resolved transient absorption decays of the T_1 to T_n transition of the annihilators, and Fig. 3d displays the time resolved upconverted emission of the annihilators. The bimolecular TTA rate constants were obtained by fitting these decay curves using eqn (3) and (4).[55,57] TTA can only occur within the closely bound triplet pair, which is formed when two annihilators in their excited triplet state meet.[58–61] The effective interaction radius follows the Einstein–Smoluchowski relation (Note S1.7, ESI†), and can be calculated from eqn (5).[62,63]

$$k_{TTA} = 4\pi DNR_{TTA} \quad (5)$$

where D is the molecular diffusion coefficient (eqn (S3), ESI†), and N is the Avogadro constant, R_{TTA} is the effective TTA reaction radius. A large molecular size due to alkyl substitution reduces the mobility of annihilator molecules and also restricts the formation of an effective triplet pair by steric hindrance. Table 1 lists the calculated TTA-UC parameters of all four annihilators. The TTA rate constants and effective radii decrease with size of the alkyl substituents. Substitution with big alkyl groups is then unfavourable for TTA kinetics for the above two reasons.

Given the negative effect of large steric substituents on the rate of TTA, the TTA efficiency can be compensated by the reduced intrinsic decay of the triplet annihilator. In a typical TTA-UC process, TTA is competing with the intrinsic decay of triplet annihilators, and the TTA quantum yield (Φ_{TTA}) follows eqn (6)

$$\Phi_{TTA} = \eta_{TTA}\left(\frac{k_{TTA}[^3A^*]}{2k_{TTA}[^3A^*] + k_T}\right) \quad (6)$$

where η_{TTA} is the possibility of TTA forming a singlet excited state according to spin statistics. Since the maximum upconversion quantum yields are at the same level, we assume the same spin statistical parameters for the four annihilators. The quantum yield of TTA is then determined by the competition between TTA and the intrinsic decay of excited triplet annihilators. Previous reports have pointed out that the radiative decay rate constant of perylene is less than 100 s^{-1}.[64] However, perylene has a high inclination to aggregate and decay non-radiatively, which increases the effective k_T.[65] We noticed that the intrinsic rate of decay decreases in the alkylated derivatives as compared to perylene, leading to an improved performance of alkylated perylene as TTA-UC annihilators.

Conclusions

Here, we have examined the TTA-UC performance of perylene and alkyl-perylene derivatives. The comparison revealed that mono-substitution with small alkyl group is sufficient in order to prevent excimer emission, while maintaining high performance. Furthermore, we demonstrate computationally

Table 1 Dynamic parameters of perylene and perylene derivatives for TTA-UC, observed and calculated from Fig. 3 and Fig. S4 (ESI)

Molecule	K_{SV}/M^{-1}	$k_{TET}/M^{-1}\ s^{-1}$	λ (T_1–T_n)/nm	ε (T_1–T_n)/$M^{-1}\ cm^{-1}$	$k_{TTA}/M^{-1}\ s^{-1}$	k_T/s^{-1}	$D/m^2\ s^{-1}$	R_{TTA}/Å
pery	9.06×10^4	2.77×10^9	485	13 400	8.40×10^9	3.55×10^3	1.72×10^{-9}	6.62
et-pery	4.43×10^4	1.26×10^9	497	11 369	5.58×10^9	1.35×10^3	1.56×10^{-9}	4.57
***t*-bu-pery**	3.70×10^4	1.05×10^9	501	11 995	5.82×10^9	1.79×10^3	1.44×10^{-9}	5.17
t-*t*-bu-pery	8.61×10^3	2.44×10^8	486	14 939	1.15×10^9	5.42×10^2	1.02×10^{-9}	1.52

how alkyl substitution prevents excimer formation on both singlet and triplet surfaces. Considering that the excess steric effect reduces the TTA-UC efficiency by restricting triplet–triplet energy transfer, a proper level of steric hindrance benefits TTA-UC systems. Furthermore, from the efficiency of annihilation it is also clear that triplet pair formation is much less sensitive to geometrical constraints than excimer formation. This comparative study thus leads to design rules for TTA-UC systems with high efficiency and contributes to the development of solar energy conversion.

Author contributions

C. Y. and K. B. conceived the project and wrote the manuscript. C. Y. carried out all the photon upconversion experiments and spectroscopy measurements. K. K. synthesized the four annihilator molecules. C. Y. and V. G. carried out all the analysis for spectroscopy. S. K. S. and P. E. carried out the quantum chemistry calculation of the energetics of annihilator dimers. All authors joined discussion and contributed to improvement of the manuscript.

Conflicts of interest

There are no conflicts to declare.

Acknowledgements

We gratefully acknowledge financial support from the Swedish Research council (2016-03354), the European Research council (ERC-2017-StG-757733), and the Knut and Alice Wallenberg Foundation. VG acknowledges funding from the Swedish research council, Vetenskapsrådet 2018-00238. C. Y. and K. B. gratefully acknowledge Dr Christoph Kerzig for proof reading and useful discussion.

References

1 V. Gray, D. Dzebo, M. Abrahamsson, B. Albinsson and K. Moth-Poulsen, *Phys. Chem. Chem. Phys.*, 2014, **16**, 10345–10352.
2 M. J. Tayebjee, D. R. McCamey and T. W. Schmidt, *J. Phys. Chem. Lett.*, 2015, **6**, 2367–2378.
3 T. F. Schulze and T. W. Schmidt, *Energy Environ. Sci.*, 2015, **8**, 103–125.
4 L. Frazer, J. K. Gallaher and T. W. Schmidt, *ACS Energy Lett.*, 2017, **2**, 1346–1354.
5 Y. Zeng, J. Chen, T. Yu, G. Yang and Y. Li, *ACS Energy Lett.*, 2017, **2**, 357–363.
6 T. Dilbeck and K. Hanson, *J. Phys. Chem. Lett.*, 2018, **9**, 5810–5821.
7 V. Gray, K. Moth-Poulsen, B. Albinsson and M. Abrahamsson, *Coord. Chem. Rev.*, 2018, **362**, 54–71.
8 Y. Y. Cheng, B. Fückel, R. W. MacQueen, T. Khoury, R. G. C. R. Clady, T. F. Schulze, N. J. Ekins-Daukes, M. J. Crossley, B. Stannowski, K. Lips and T. W. Schmidt, *Energy Environ. Sci.*, 2012, **5**, 6953–6959.
9 V. Jankus, E. W. Snedden, D. W. Bright, V. L. Whittle, J. A. G. Williams and A. Monkman, *Adv. Funct. Mater.*, 2013, **23**, 384–393.
10 A. Monguzzi, D. Braga, M. Gandini, V. C. Holmberg, D. K. Kim, A. Sahu, D. J. Norris and F. Meinardi, *Nano Lett.*, 2014, **14**, 6644–6650.
11 A. Monguzzi, S. M. Borisov, J. Pedrini, I. Klimant, M. Salvalaggio, P. Biagini, F. Melchiorre, C. Lelii and F. Meinardi, *Adv. Funct. Mater.*, 2015, **25**, 5617–5624.
12 S. P. Hill, T. Dilbeck, E. Baduell and K. Hanson, *ACS Energy Lett.*, 2016, **1**, 3–8.
13 S. P. Hill and K. Hanson, *J. Am. Chem. Soc.*, 2017, **139**, 10988–10991.
14 B. Shan, T.-T. Li, M. K. Brennaman, A. Nayak, L. Wu and T. J. Meyer, *J. Am. Chem. Soc.*, 2019, **141**, 463–471.
15 K. Börjesson, D. Dzebo, B. Albinsson and K. Moth-Poulsen, *J. Mater. Chem. A*, 2013, **1**, 8521–8524.
16 C. Kerzig and O. S. Wenger, *Chem. Sci.*, 2018, **9**, 6670–6678.
17 D. Choi, S. K. Nam, K. Kim and J. H. Moon, *Angew. Chem., Int. Ed.*, 2019, **58**, 6891–6895.
18 B. D. Ravetz, A. B. Pun, E. M. Churchill, D. N. Congreve, T. Rovis and L. M. Campos, *Nature*, 2019, **565**, 343–346.
19 Y.-H. Chen, C.-C. Lin, M.-J. Huang, K. Hung, Y.-C. Wu, W.-C. Lin, R.-W. Chen-Cheng, H.-W. Lin and C.-H. Cheng, *Chem. Sci.*, 2016, **7**, 4044–4051.
20 K. Börjesson, P. Rudquist, V. Gray and K. Moth-Poulsen, *Nat. Commun.*, 2016, **7**, 12689.
21 J. Han, P. Duan, X. Li and M. Liu, *J. Am. Chem. Soc.*, 2017, **139**, 9783–9786.
22 R. Vadrucci, A. Monguzzi, F. Saenz, B. D. Wilts, Y. C. Simon and C. Weder, *Adv. Mater.*, 2017, **29**, 1702992.
23 D. Yang, J. Han, M. Liu and P. Duan, *Adv. Mater.*, 2018, **0**, 1805683.
24 X. Yang, J. Han, Y. Wang and P. Duan, *Chem. Sci.*, 2019, **10**, 172–178.
25 Q. Liu, T. Yang, W. Feng and F. Li, *J. Am. Chem. Soc.*, 2012, **134**, 5390–5397.
26 Q. Liu, W. Feng, T. Yang, T. Yi and F. Li, *Nat. Protoc.*, 2013, **8**, 2033.
27 Q. Liu, B. Yin, T. Yang, Y. Yang, Z. Shen, P. Yao and F. Li, *J. Am. Chem. Soc.*, 2013, **135**, 5029–5037.
28 O. S. Kwon, H. S. Song, J. Conde, H.-i. Kim, N. Artzi and J.-H. Kim, *ACS Nano*, 2016, **10**, 1512–1521.
29 S. Mattiello, A. Monguzzi, J. Pedrini, M. Sassi, C. Villa, Y. Torrente, R. Marotta, F. Meinardi and L. Beverina, *Adv. Funct. Mater.*, 2016, **26**, 8447–8454.
30 J. Park, M. Xu, F. Li and H.-C. Zhou, *J. Am. Chem. Soc.*, 2018, **140**, 5493–5499.
31 D. Yildiz, C. Baumann, A. Mikosch, A. J. C. Kuehne, A. Herrmann and R. Gostl, *Angew. Chem., Int. Ed.*, 2019, **58**, 12919–12923.
32 M. Kitazawa, T. Yabe, Y. Hirata and T. Okada, *J. Mol. Liq.*, 1995, **65–66**, 321–324.
33 R. Casillas, M. Adam, P. B. Coto, A. R. Waterloo, J. Zirzlmeier, S. R. Reddy, F. Hampel, R. McDonald,

R. R. Tykwinski, M. Thoss and D. M. Guldi, *Adv. Energy Mater.*, 2019, **9**, 1802221.
34 J. H. Schön, C. Kloc and B. Batlogg, *Appl. Phys. Lett.*, 2000, **77**, 3776–3778.
35 J.-H. Kim, F. Deng, F. N. Castellano and J.-H. Kim, *ACS Photonics*, 2014, **1**, 382–388.
36 C. Li, C. Koenigsmann, F. Deng, A. Hagstrom, C. A. Schmuttenmaer and J.-H. Kim, *ACS Photonics*, 2016, **3**, 784–790.
37 S. Hoseinkhani, R. Tubino, F. Meinardi and A. Monguzzi, *Phys. Chem. Chem. Phys.*, 2015, **17**, 4020–4024.
38 A. J. Musser, S. K. Rajendran, K. Georgiou, L. Gai, R. T. Grant, Z. Shen, M. Cavazzini, A. Ruseckas, G. A. Turnbull, I. D. W. Samuel, J. Clark and D. G. Lidzey, *J. Mater. Chem. C*, 2017, **5**, 8380–8389.
39 C. B. Dover, J. K. Gallaher, L. Frazer, P. C. Tapping, A. J. Petty, M. J. Crossley, J. E. Anthony, T. W. Kee and T. W. Schmidt, *Nat. Chem.*, 2018, **10**, 305–310.
40 C. Ye, V. Gray, J. Mårtensson and K. Börjesson, *J. Am. Chem. Soc.*, 2019, **141**, 9578–9584.
41 J. Shi and C. W. Tang, *Appl. Phys. Lett.*, 2002, **80**, 3201–3203.
42 B. K. Shah, D. C. Neckers, J. Shi, E. W. Forsythe and D. Morton, *J. Phys. Chem. A*, 2005, **109**, 7677–7681.
43 V. Gray, A. Dreos, P. Erhart, B. Albinsson, K. Moth-Poulsen and M. Abrahamsson, *Phys. Chem. Chem. Phys.*, 2017, **19**, 10931–10939.
44 K. Kushwaha, L. Yu, K. Stranius, S. K. Singh, S. Hultmark, M. N. Iqbal, L. Eriksson, E. Johnston, P. Erhart, C. Muller and K. Börjesson, *Adv. Sci.*, 2019, **6**, 1801650.
45 J. Yang, A. Dass, A.-M. M. Rawashdeh, C. Sotiriou-Leventis, M. J. Panzner, D. S. Tyson, J. D. Kinder and N. Leventis, *Chem. Mater.*, 2004, **16**, 3457–3468.
46 A. Monguzzi and J. Pedrini, *J. Photonics Energy*, 2017, **8**, 022005.
47 V. Gray, D. Dzebo, M. Abrahamsson, B. Albinsson and K. Moth-Poulsen, *Phys. Chem. Chem. Phys.*, 2014, **16**, 10345–10352.
48 T. N. Singh-Rachford and F. N. Castellano, *J. Phys. Chem. Lett.*, 2010, **1**, 195–200.
49 C. Lee, W. Yang and R. G. Parr, *Phys. Rev. B: Condens. Matter Mater. Phys.*, 1988, **37**, 785–789.
50 L. A. Curtiss, P. C. Redfern and K. Raghavachari, *J. Chem. Phys.*, 2005, **123**, 124107.
51 S. Grimme, J. Antony, S. Ehrlich and H. Krieg, *J. Chem. Phys.*, 2010, **132**, 154104.
52 B. Karpichev, L. Koziol, K. Diri, H. Reisler and A. I. Krylov, *J. Chem. Phys.*, 2010, **132**, 114308.
53 O. Bludský, M. Rubeš, P. Soldán and P. Nachtigall, *J. Chem. Phys.*, 2008, **128**, 114102.
54 X. Liu and J. Qiu, *Chem. Soc. Rev.*, 2015, **44**, 8714–8746.
55 C. Bohne, E. B. Abuin and J. C. Scaiano, *J. Am. Chem. Soc.*, 1990, **112**, 4226–4231.
56 T. W. Schmidt and F. N. Castellano, *J. Phys. Chem. Lett.*, 2014, **5**, 4062–4072.
57 J. Saltiel, G. R. March, W. K. Smothers, S. A. Stout and J. L. Charlton, *J. Am. Chem. Soc.*, 1981, **103**, 7159–7164.
58 S. Baluschev, V. Yakutkin, G. Wegner, B. Minch, T. Miteva, G. Nelles and A. Yasuda, *J. Appl. Phys.*, 2007, **101**, 023101.
59 T. L. Keevers and D. R. McCamey, *Phys. Rev. B*, 2016, **93**, 045210.
60 B. S. Basel, J. Zirzlmeier, C. Hetzer, S. R. Reddy, B. T. Phelan, M. D. Krzyaniak, M. K. Volland, P. B. Coto, R. M. Young, T. Clark, M. Thoss, R. R. Tykwinski, M. R. Wasielewski and D. M. Guldi, *Chem*, 2018, **4**, 1092–1111.
61 K. Miyata, F. S. Conrad-Burton, F. L. Geyer and X. Y. Zhu, *Chem. Rev.*, 2019, **119**, 4261–4292.
62 J. Keizer, *Chem. Rev.*, 1987, **87**, 167–180.
63 B. Nickel, P. Borowicz, A. A. Ruth and J. Troe, *Phys. Chem. Chem. Phys.*, 2004, **006**, 3350–3363.
64 P. J. Walla, F. Jelezko, P. Tamarat, B. Lounis and M. Orrit, *Chem. Phys.*, 1998, **233**, 117–125.
65 Y. Hong, J. W. Y. Lam and B. Z. Tang, *Chem. Soc. Rev.*, 2011, **40**, 5361–5388.

Electronic Supplementary Material (ESI) for Physical Chemistry Chemical Physics.

Supporting Information for

Optimizing photon upconversion by decoupling excimer formation and triplet triplet annihilation

Chen Ye,[a] Victor Gray,[b,c] Khushbu Kushwaha,[a] Sandeep Kumar Singh,[d] Paul Erhart,[d] and Karl Börjesson[a]*

AUTHOR ADDRESS

a Dr. C. Ye, Dr. K. Kushwaha, Dr. K. Börjesson
Department of Chemistry and Molecular Biology, University of Gothenburg, 41296 Gothenburg, Sweden.
E-mail: karl.borjesson@gu.se

b Dr. V. Gray
Department of Chemistry–Ångström Laboratory, Uppsala University, 75120, Uppsala, Sweden.

c Dr. V. Gray
Department of Physics, Cavendish Laboratory, University of Cambridge, 19 JJ Thompson Avenue, Cambridge, CB3 0HE, UK.

d Dr. S. K. Singh, Prof. Dr. P. Erhart
Department of Physics, Chalmers University of Technology, 41296 Gothenburg, Sweden.

1. Experimental Section

1.1 TTA-UC sample preparation

All TTA-UC samples were prepared in an Mbraun glove box having oxygen and water levels less than 1 ppm. Cuvettes were sealed with cap and PTFE septum. Photon upconversion measurements were performed immediately after the preparation.

1.2 Steady state emission

Steady state emission of TTA-UC samples with PtTBTP was measured on an Edinburgh Instruments FLS 1000 spectrofluorometer. A Light Emitting Diode (LED) with collimator and focus lenses was used as a non-coherent excitation source. Emission was collected 90 degrees as compared to the excited light. The LED light source (617 nm, Thorlabs M617L3 mounted LED), power supply and all the optical units were purchased from Thorlabs, Inc. The connection and supporting units were home-made from non-fluorescent plastic[2] by 3D-printing.

1.3 Quantum yield calculations.

The photoluminescence quantum yield of the luminescent species were determined from an indirect method with standard reference as recommend by IUPAC.[3] The quantum yield of the testing samples (Φ_S) were calculated by the following equation:

$$\Phi_S = \Phi_R \times \frac{\int F_S(\lambda)\, d\lambda}{\int F_R(\lambda)\, d\lambda} \times \left(\frac{n_S}{n_R}\right)^2 \times \frac{I_R}{I_S} \times \frac{1 - 10^{-A_R}}{1 - 10^{-A_S}} \quad (eq.S1)$$

where Φ_R is the fluorescence quantum yield of the reference sample, $F_i(\lambda)$ is the emission intensity function, n_i is the refractive index of the solvent, I_i is the excitation intensity, and A_i is the absorbance of the sample at the excitation wavelength. Standard reference materials were selected by the excitation and emission spectrum range according to

IUPAC recommendations. Quinine sulphate in H_2SO_4 solution was used as reference for calculating the fluorescence quantum yields of perylene derivatives (Φ_R = 0.52). Cresyl violet was used as reference for calculating the photon upconversion quantum yields (Φ_R = 0.57). For TTA-UC with perylene as the annihilator, the emission of monomer is integrated from 400 to 540 nm, due to the low intensity of perylene monomer emission outside this range. The excimer emission is integrated from 540 nm to 700 nm.

1.4 Time resolved spectroscopy

Phosphorescence quenching was measured on an Edinburgh FLS 1000 spectrofluorometer with a microsecond flash lamp as excitation source. Prompt fluorescence decay was recorded by time-correlated single photon counting (TCSPC) on Edinburgh FLS 1000 spectrofluorometer with a pulsed diode laser (375 nm, 1 MHz) as the excitation source and MCP-PMT as detector. Phosphorescence and delayed fluorescence decays were recorded by time-correlated single photon counting on Edinburgh FLS 1000 spectrofluorometer with a pulsed diode laser (375 nm, 1 MHz) as the excitation source and MCP-PMT as the detector. Fluorescence decay was recorded by multi-channel scaling (MCS) on Edinburgh FLS 1000 spectrofluorometer with a pulsed microsecond flash lamp (617 nm, 100 Hz) as the excitation source and PMT-900 as the detector.

Transient absorption was measured on an Edinburgh Instrument LP 980 spectrometer, with a Spectra-Physics Nd:YAG laser (617 nm, pulse width ~7 ns) coupled to a Spectra-Physics primoscan optical parametric oscillator (OPO) as excitation. PMT (Hamamatsu R928) or image intesified CCD camera (ICCD, Andor DH320T-25F-03) detectors were used for recording transient kinetics or spectra, respectively.

1.5 Rate determination step of TET

TET from the sensitizer involves diffusion and energy transfer. The diffusion constant k_{diff} is estimated by the following equation:

$$k_{diff} = \frac{8RT}{3\eta} \quad (eq.S2)$$

where *R* is the ideal gas constant, *T* is the absolute temperate, η is the viscosity of the solvent. The k_{diff} is 1.4×10^{10} $M^{-1}s^{-1}$ at room temperature in THF. The calculated k_{TET} is smaller than k_{diff}, and thus the quenching is TET limited.

1.6 Density functional theory (DFT) calculations.

The effect of excitations on the interaction between a pair of perylene molecules was analysed within the framework of time-dependent density functional theory (TDDFT). Calculations were carried out using the B3LYP functional[4] with dispersion corrections (D3BJ)[5] and the 6−311G* basis set[6] as implemented in the NWChem suite[7]. This approach closely follows our earlier calculations[1].

1.7 The effective and average TTA reaction radii of perylene and perylene derivatives.

Diffusion coefficients (*D*) in solutions can be calculated by the empirical correlation developed by Wilke Chang.[8]

$$D = 7.4 \times 10^{-8} \frac{(xM)^{0.5}T}{\eta V^{0.6}} \quad (eq.S3)$$

where *x* is the association number of solvent, M is the molecular weight of solute, T is the temperature, η is the viscosity of the solvent, and V is the molecular volume of the solvent.

Based on the analysis of time resolved spectroscopy, we got the apparent kinetic parameters (k_{TTA}, k_T, R_{TTA}) for TTA with the different annihilators. To compare the four annihilators, we want to calculate the mean TTA interaction distance (d_{TTA}). The TTA time window relies on the lifetime, which greatly exceeds the diffusion time character ($\tau >> R_{TTA}^2/D$). We can treat the distribution of triplet excited annihilator through diffusion as a fast process before TTA. Triplet-triplet annihilation is a typical case of a bi-molecular photophyscial transformation, which involves the diffusion of excited species. In our work, we show the difference of four annihilator molecules on TTA-UC and discuss the advantages and disadvantages of alkylation of perylene on TTA-UC. To make the mechanism more clear and intuitive, we want to take the relative motion of two triplet excited species into account in the analysis. We treat the first triplet excited annihilator as stationary, as a nearby second triplet excited annihilator approaches. The relative motion of the mobile component to the static component follows Fick's second law of diffusion with an interaction term (eq. S4):

$$\frac{\partial \rho}{\partial t} = D\nabla^2\rho - k_T\rho - 2k_{TTA}\rho^2 \quad (eq.S4)$$

where $\rho = C/C_0$ is the time and spatial dependent density (normalized concentration) of the triplet excited annihilator, and $\nabla = \partial/\partial \mathrm{r}$ is the Laplace operator in radial coordinates. When approximating steady state conditions, we assume a spatially independent density ($D\nabla^2\rho = 0$), which reduces eq. S4 to an ordinary differential equation (eq. 3; Figure 3c). To take the spatial distribution of molecules into account in eq S2, we assume that TTA is a diffusion limited process (eq. S5):

$$\frac{\partial \rho}{\partial t} = D\frac{\partial^2 \rho}{\partial r^2} \quad (eq.S5)$$

The annihilator interaction range ($r = R_{TTA}$) is the intermolecular distance for complete TTA reaction (100% efficient trapping). At the initial time, the reacting molecules are randomly distributed with a uniform concentration outside the complete reaction zone. Given that TET is fast and efficient, the boundary conditions of a statistical distribution outside the annihilator interaction range can be described as below:

$$\rho_{(r,t=0)} = 0 \text{ for } r \leq R_{TTA}$$

$$\rho_{(r,t=0)} = 1 \text{ for } r > R_{TTA}$$

Marian Smoluchowski found the solution of eq. S3 with the above Dirichlet boundary conditions,[9]

$$\rho(r,t) = 1 - \frac{R_{TTA}}{r}\,\mathrm{erfc}\left[\frac{r - R_{TTA}}{2\sqrt{DT}}\right] \quad (eq.S6)$$

$$\rho(r,\infty) = 1 - \frac{R_{TTA}}{r} \quad (eq.S7)$$

where erfc(x) is the complementary error function. With increasing time, the distribution function turns to a steady-state expression (eq. S7). As shown in figure below, the distribution of triplet excited annihilators reach stationary conditions at the beginning of the TTA process, indicating that our approximation is reasonable.

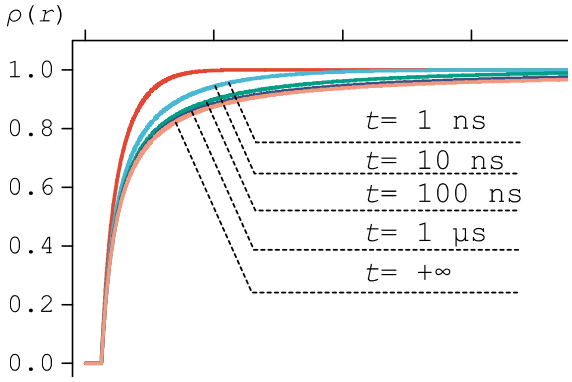

Normalized theoretical density of triplet excited annihilator as a function of intermolecular distance at different times after triplet formation.

The reaction rate of TTA is based on the flux of molecules at the encounter distance. The apparent rate constant of TTA then satisfies the following expression (eq. S8):

$$k_{TTA} = 4\pi N R_{TTA}^2 D \frac{\partial \rho(r)}{\partial r} = 4\pi D N R_{TTA}\left[1 + \frac{R_{TTA}}{(\pi D t)^{1/2}}\right] \quad (eq.S8)$$

where at the TTA time scale, t is much larger than the diffusion characteristic time R_{TTA}^2/D, and the rate equation converts to the steady-state expression (eq. 5; Table 1). TTA is a special case of Dexter energy transfer, in which excited electrons are transferred between two annihilator molecules via a non-radiative path. The Dexter energy transfer process requires enough overlap between the two electron clouds, and it is thus only effective within a very short range (~10 Å).[10] The annihilation rate constant therefore follow the Dexter energy transfer formulation (eq. S9):[11]

$$k_{Dex}(r) = k_0 exp\left(\frac{-2r}{L}\right) \quad (eq.S9)$$

where *L* is average Bohr radius of the chromophores. The Dexter energy transfer rate decreases dramatically when increasing the donor-acceptor distance. Based on this, we can calculate the spatially dependent TTA reaction possibility by the following formula (eq. S10):

$$\rho_r(r) = \frac{k_{Dex}(r)}{k_0}\rho(r) \quad (eq.S10)$$

The steady-state distribution and TTA reaction probability is shown below. By integrating the reaction probability in radial coordinates, we calculated the mean TTA interaction distance of **pery**, **et-pery**, ***t*-bu-pery** and **t-*t*-bu-pery** to be 1.44 nm, 1.26 nm, 1.31 nm, and 1.03 nm, respectively (eq. S11). From these numbers it is clear that large steric groups reduce the active zone for TTA interaction, and is thus unfavourable for building efficient TTA-UC systems. The trend for the mean TTA interaction (d_{TTA}) also follows the effective interaction (R_{TTA}, Table 1).

$$d_{TTA} = \frac{\int_{R_{TTA}}^{\infty} 4\pi r^2\, \rho_r(r)\, r\, dr}{\int_{R_{TTA}}^{\infty} 4\pi r^2\, \rho_r(r)\, dr} \quad (eq.S11)$$

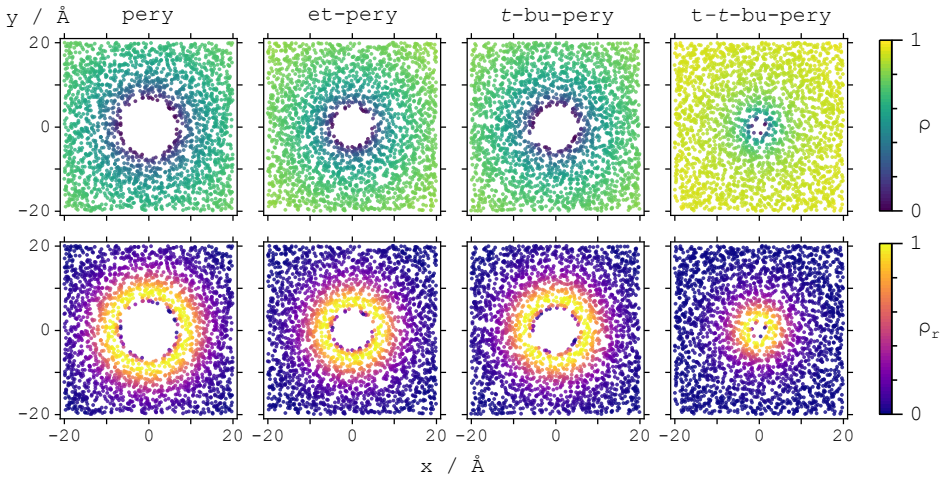

Normalized theoretical density of triplet excited annihilator around a fixed annihilator and the corresponding normalized TTA reaction probability by Monte Carlo simulations under steady-state approximations.

2. Figures cited in the main text.

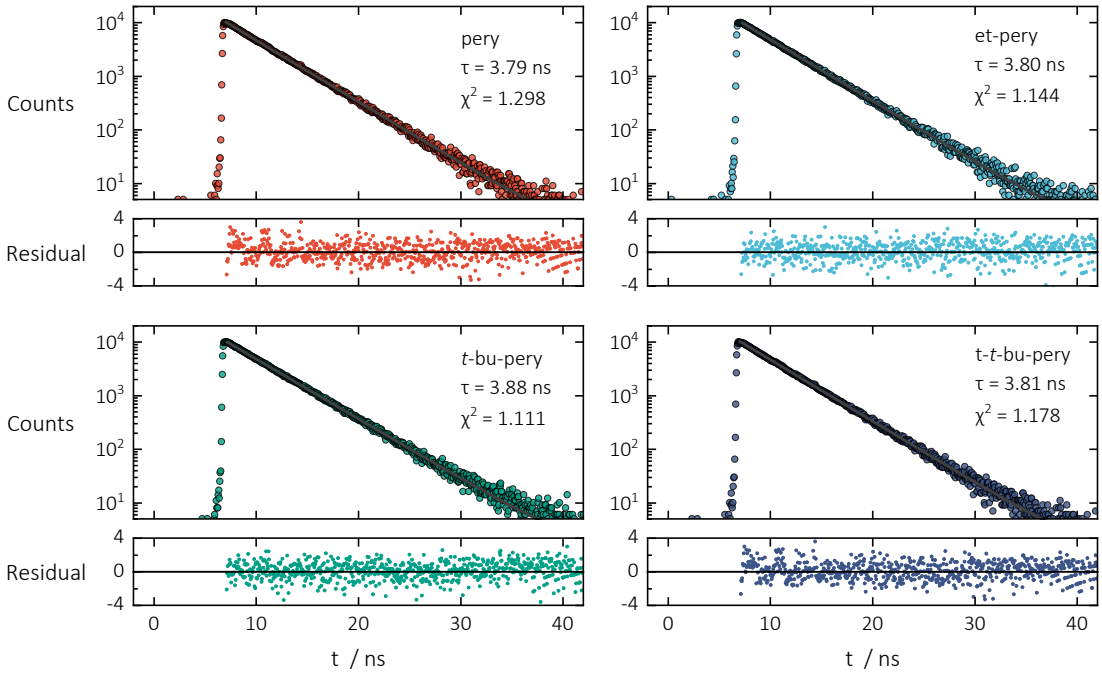

Figure S1. Time resolved photoluminescence decay of perylene and perylene derivatives (10 μM) in THF. The excitation and detection wavelengths are 375 nm and 445 nm, respectively.

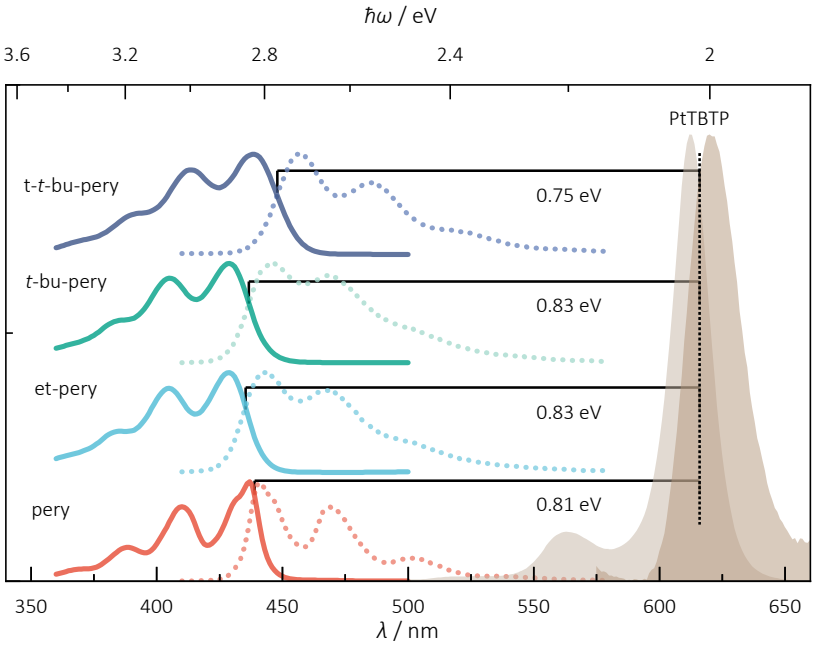

Figure S2. Absorption and emission spectrum of **PtTBTP**, **pery**, **et-pery**, ***t*-bu-pery** and **t-*t*-bu-pery** in THF. Stokes shifts are labelled as the differences of E_{00} values from annihilators to sensitizer. Note that the porphyrin emission is the weak fluorescence signal from this molecule.

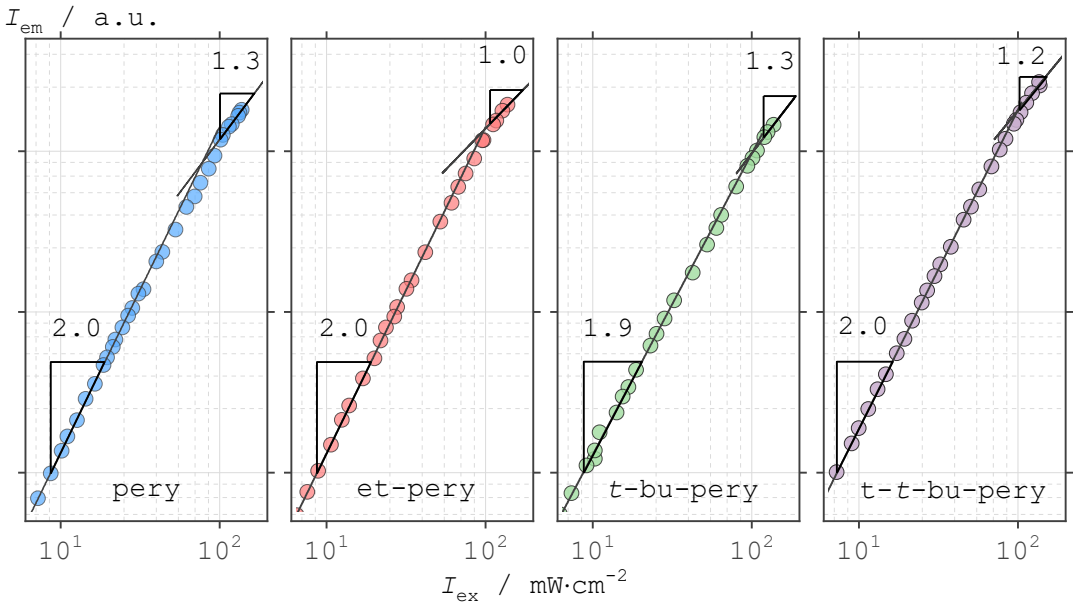

Figure S3. Upconversion intensity of 10 μM sensitizer and 1 mM annihilator in THF at different excitation power

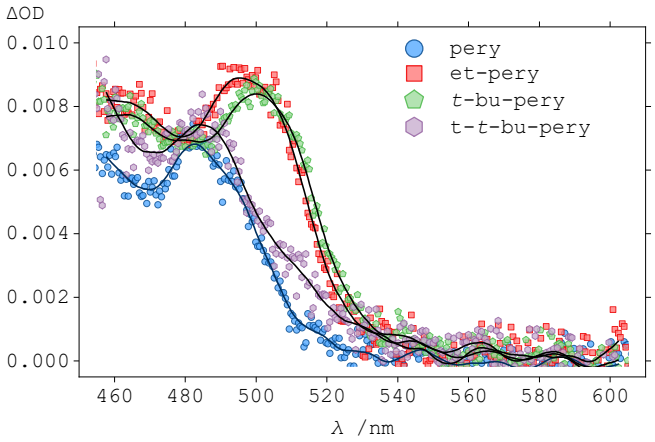

Figure S4. Transient absorption spectrum of 1mM **pery**, **et-pery**, ***t*-bu-pery** and **t-*t*-bu-pery** in THF with 10 µM PtTBTP as sensitizer. All these samples are excited at 617 nm.

3. References

[1] K. Kushwaha, L. Yu, K. Stranius, S. K. Singh, S. Hultmark, M. N. Iqbal, L. Eriksson, E. Johnston, P. Erhart, C. Muller, K. Börjesson, *Adv. Sci.* **2019**, *6*, 1801650.

[2] B. Joarder, N. Yanai, N. Kimizuka, *J. Phys. Chem. Lett.* **2018**, *9*, 4613-4624.

[3] A. M. Brouwer, *Pure Appl. Chem.* **2011**, *83*, 2213-2228.

[4] a) C. Lee, W. Yang, R. G. Parr, *Phys. Rev. B* **1988**, *37*, 785-789; b) A. D. Becke, *J. Chem. Phys.* **1993**, *98*, 5648-5652.

[5] S. Grimme, J. Antony, S. Ehrlich, H. Krieg, *J. Chem. Phys.* **2010**, *132*, 154104.

[6] a) A. D. McLean, G. S. Chandler, *J. Chem. Phys.* **1980**, *72*, 5639-5648; b) R. Krishnan, J. S. Binkley, R. Seeger, J. A. Pople, *J. Chem. Phys.* **1980**, *72*, 650-654.

[7] M. Valiev, E. J. Bylaska, N. Govind, K. Kowalski, T. P. Straatsma, H. J. J. Van Dam, D. Wang, J. Nieplocha, E. Apra, T. L. Windus, W. A. de Jong, *Comput. Phys. Commun.* **2010**, *181*, 1477-1489.

[8] C. R. Wilke, P. Chang, *AIChE J.* **1955**, *1*, 264-270.

[9] M. v. Smoluchowski, *Z. Phys. Chem.* **1918**, *92*, 129.

[10] T. Mirkovic, E. E. Ostroumov, J. M. Anna, R. van Grondelle, Govindjee, G. D. Scholes, *Chem. Rev.* **2017**, *117*, 249-293.

[11] S. Faure, C. Stern, R. Guilard, P. D. Harvey, *J. Am. Chem. Soc.* **2004**, *126*, 1253-1261.